Bestrophin-2 Is Involved in the Generation of Intraocular Pressure

Benjamin Bakall,[1] Precious McLaughlin,[1] J. Brett Stanton,[1] Youwen Zhang,[1] H. Criss Hartzell,[2] Lihua Y. Marmorstein,[1,3] and Alan D. Marmorstein[1,4]

PURPOSE. The bestrophin family of proteins has been demonstrated to generate or regulate Ca^{2+}-activated Cl^- conductances. Mutations in bestrophin-1 (*Best1*) cause several blinding eye diseases, but little is known about other bestrophin family members. This study involved disruption of the *Best2* gene in mice.

METHODS. The mouse *Best2* gene was disrupted by replacing exons 1, 2, and part of exon 3 with a *Lac Z*. The expression profile of Bestrophin-2 (Best2) was examined using RT-PCR, X-gal staining, and immunohistochemistry. Intraocular pressure (IOP) was measured by anterior chamber cannulation.

RESULTS. RT-PCR of mouse tissues revealed *Best2* mRNA in eye, colon, nasal epithelia, trachea, brain, lung, and kidney. X-gal staining, confirmed expression in colon epithelia and in the eye, in the nonpigmented epithelia (NPE). *Best2* was not expressed in RPE cells. Best2 protein was observed only in NPE and colon epithelia. The absence of *Best2* had no obvious deleterious effect on the mice. However, the $Best2^{-/-}$ mice were found to have significantly ($P < 0.02$) diminished IOP with respect to the $Best2^{+/+}$ and $Best2^{+/-}$ littermates. The $Best2^{-/-}$ and $Best2^{+/-}$ mice responded better to the carbonic anhydrase inhibitor brinzolamide than did their $Best2^{+/+}$ littermates, although the β-blocker timolol brought IOP to the same level, regardless of genotype.

CONCLUSIONS. Best2 plays a role in the generation of IOP by regulating formation of aqueous humor, and inhibition of Best2 function represents an attractive new avenue for regulating IOP in individuals with glaucoma. (*Invest Ophthalmol Vis Sci.* 2008;49:1563–1570) DOI:10.1167/iovs.07-1338

Bestrophins are a recently recognized family of proteins linked to Ca^{2+} sensitive Cl^- transport.[1,2] It is clear on the basis of multiple studies that these proteins play an important role in Ca^{2+}-sensitive Cl^- transport, although they may have other functions as well.[1,2] There are four bestrophin genes in

mammals, designated *Best1* through *Best4*.[3] The genes were originally designated *VMD2 (Best1)* and *VMD2L1* through *VMD2L3*. *Best4* (formerly designated *VMD2L2*) is a pseudogene in mice, and there is no evidence that the gene is functionally expressed in humans.[4] *Best1*, is the prototypic member of the bestrophin family in mammals. Mutations in human *BEST1* are causally associated with the blinding eye diseases Best vitelliform macular dystrophy (BVMD, OMIM 153700; Online Mendelian Inheritance in Man; http://www.ncbi.nlm.nih.gov/Omim/ provided in the public domain by the National Center for Biotechnology Information, Bethesda, MD), Adult-onset vitelliform macular dystrophy (OMIM 608161), and autosomal dominant vitreoretinochoroidopathy (OMIM 193220).[2] All three diseases exhibit dominant inheritance and with only a few exceptions, all the disease-causing mutations are either missense or single amino acid deletions.

The association of human *Best1* with BVMD, a disease characterized by a diminished electrooculogram light peak,[5,6] a response generated by activation of a Ca^{2+}-sensitive Cl^- conductance,[7] led to the hypothesis that bestrophins are Cl^- channels.[8] Best1 is an integral membrane protein that forms dimers and potentially higher-order oligomers.[9] All mammalian bestrophins are predicted to have at least four transmembrane domains, a structure that is supported with experimental data for Best1.[10,11] Heterologous expression of bestrophins results in the de novo activation of Cl^- currents with unique, bestrophin-specific, I/V relationships.[8] Best2-associated Cl^- currents are perhaps the best characterized.[12–14] Extensive mutagenesis of the second transmembrane domain in Best2 has identified amino acid residues that appear to confer ion selectivity, suggesting that bestrophins can form channel pores.[13,14] However, the disruption of mouse *Best1* does not diminish the light peak, nor does it cause obvious changes in Ca^{2+}-sensitive Cl^- conductances measured in freshly isolated RPE cells.[15] In addition, expression of human BEST1 and disease causing mutants in RPE-J cells results in changes in the kinetics of voltage-dependent Ca^{2+} channels.[16] Studies in which VDCC (voltage-dependent Ca^{2+} channel) inhibitors have been used, and mice in which VDCC subunits are disrupted, have demonstrated that VDCCs are necessary for proper generation of the light peak response in mice and rats.[15–17] Taken together, these data suggest that bestrophins may not generate Ca^{2+}-sensitive Cl^- conductances but may be involved in regulating Ca^{2+} signaling.

In an effort to gain a better understanding of the role of bestrophins, we characterized a mouse in which the *Best2* gene was disrupted by targeted insertion of the *LacZ* gene. In addition to ablating expression of Best2, the *LacZ* gene is under control of the endogenous *Best2* promoter, allowing for reporter analysis of *Best2* gene expression. In this article, we report that Best2 is expressed predominantly in the nonpigmented ciliary epithelium (NPE) of the eye and in the epithelial cells of the colon. Gene expression data for these sites is confirmed by immunostaining using a well-characterized antibody against murine Best2. We found that disruption of the *Best2* gene results in a significantly diminished IOP and altered sensitivity to drugs that affect the generation of aqueous hu-

mor. Based on these findings we conclude that Best2 represents a novel target for the development of new drugs to lower IOP by diminishing aqueous inflow.

MATERIALS AND METHODS

Targeted Disruption of the Mouse *Best2* Gene and Southern Blot Analysis

The targeting vector was constructed using 0.8-kb (5′) and 2.9-kb (3′) mouse *Best2* genomic DNA fragments as homology arms. The two arms flanked a promoterless lacZ and a neomycin-resistant gene cassette (lacZ-neo). Homologous recombination in mouse embryonic stem cells resulted in the insertion of the lacZ-neo cassette, replacing a region spanning exon 1 through a part of exon 3 of the mouse *Best2* locus. Germ-line–transmitting chimeric mice generated from the targeted embryonic stem cells were bred with C57BL/6 mice to produce *Best2*$^{+/-}$ mice (Deltagen, San Mateo, CA). Intercrossing of heterozygous mice generated *Best2*$^{-/-}$ mice. Southern blot analysis was performed for identification of homologous recombinants on genomic DNA digested with *Eco*RV, separated on an 0.8% agarose gel (SeaKem Gold; Cambrex, East Rutherford, NJ) and transferred to a nylon membrane (Hybond-N^{+}; GE Healthcare, Piscataway, NJ) by capillary blotting. The membrane was hybridized with a 3′ external probe located outside of the homologous arm regions (Fig. 1A). The probes were labeled with ^{32}P via random priming with a DNA labeling system (Megaprime DNA Labeling System; GE Healthcare) and purified (Probe-Quant G-50 Micro Columns; GE Healthcare). Hybridization was performed with a commercial solution (MiracleHyb; Stratagene, La Jolla, CA), according to the manufacturer's instructions. PCR was performed for subsequent genotyping. All studies conformed to the ARVO Statement for the Use of Animals in Ophthalmic and Vision Research.

Reverse Transcription–Polymerase Chain Reaction

Reverse transcription–PCR (RT-PCR) was performed to confirm the absence of *Best2* expression in the homozygous mice. Total RNA was isolated (TRIzol; Invitrogen, Carlsbad, CA) and reverse transcribed (Superscript III; Invitrogen). A 3′ primer set corresponding to the *Best2* cDNA sequence was used in the PCR. This primer set (5′-ATGGCACTAAGCGCCGCCTATC-3′ and 5′-CTGGGTGTAGACGAGGGGTA-3′) generates a 585-bp fragment. A set of mouse fibulin-3 primers, generating a 372-bp fragment, were used as a positive control.

RT-PCR was also performed to identify expression of human *BEST1* and *BEST2* in isolated human ciliary body and RPE. Donor eyes were obtained from the Cleveland Eye Bank. The following primers sets were used: *BEST1* (5′-atgtactggaataagcccgag-3′ and 5′-ttaggaatgtgct-tcatccctg-3′), 752-bp and *BEST2* (5′-ATTGTGACCAGTATGCCAGC-CTCA-3′ and 5′-TTTCAAACTTCTTGCGCTCCTCGC-3′), 315 bp. β-Actin primers resulting in a 234-bp product were used as a control (5′-GGACTTCGAGCAAGAGATGG-3′ and 3′-AGCACTGTGTTGGCGTA-CAG-3′).

X-gal Staining

Staining for expression of the *LacZ* reporter was performed on 10-μm frozen sections of tissue fixed in 4% paraformaldehyde in PBS. Sections were postfixed for 1 minute in 2% formaldehyde, 0.2% glutaraldehyde in PBS, containing 0.1% Tween 20, rinsed twice in 100 mM Tris-HCl (pH 7.4), 100 mM NaCl, 50 mM MgCl$_2$, and 0.1% Tween 20, and incubated for 3 hours or overnight in a 1-mg/mL solution of X-gal (Tissue Stain Solution; Chemicon, Temecula, CA). After three washes in PBS containing 0.1% Tween 20, the samples were counterstained with nuclear fast red. The sections were examined with a microscope (model E-600) and photographed with a color CCD camera using ACTII software (Nikon, Tokyo, Japan).
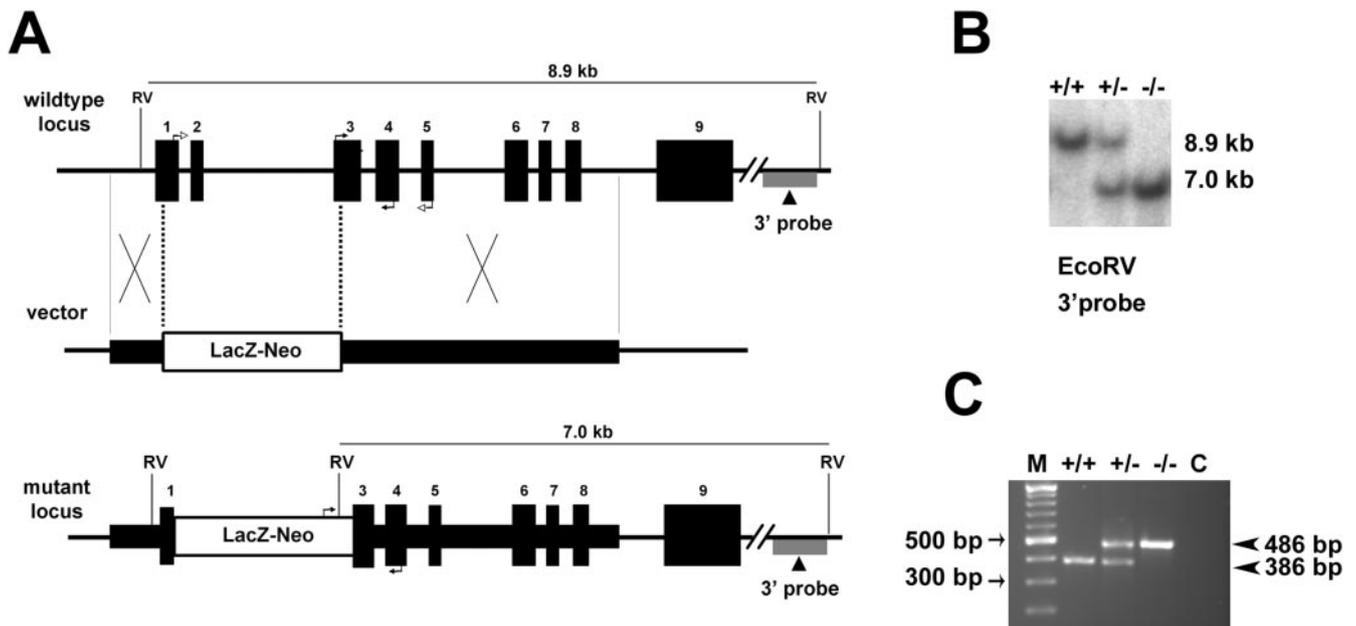

FIGURE 1. Targeted disruption of the mouse *Best2* gene. (A) The wild-type locus, targeting vector, and mutant locus. *Thick lines*: fragments used for constructing the targeting vector 5′ and 3′ arms. *Thin lines*: genomic DNA or vector backbone sequence. *Numbered solid boxes*: Best2 exons. *Labeled boxes*: the LacZ and neo^r expression cassette. The external 3′ probe used for Southern blot analysis in (B) is indicated under the wild-type and mutant loci. *Filled arrows* at exons 3 and 4 of the wild-type locus and LacZ-neo^r and exon 4 of mutant locus indicate the PCR primers used for genotyping in (C). *Open arrows* at exons 1 and 5 of wild-type locus indicate the primers used for RT-PCR in Figure 2. RV, *Eco*RV. (B) Southern Blot analysis was performed to identify homologous recombinants. Mouse genomic DNA was digested with *Eco*RV. Wild-type (+/+) fragment, 8.9 kb; mutant (−/−) fragment, 7.0 kb. The heterozygous mice (+/−) had both fragments. (C) Genotyping was confirmed using a multiplex PCR with two forward primers in exon 3 and the LacZ and neo^r expression cassette, respectively, and one reverse primer in exon 4. The 386-bp product represents the wild-type allele and is absent from the *Best2*$^{-/-}$ mice. The 486-bp product representing the disrupted allele is present only in the *Best2*$^{+/-}$ and *Best2*$^{-/-}$ mice. M, molecular weight marker.

Transfection and Western Blot Analysis

HEK293 cells were transfected with the plasmid pAdlox-mBest2 by means of a lipophilic transfection reagent (Lipofectamine; Invitrogen), as described elsewhere.[18] Forty-eight hours after transfection, the cells were lysed in SDS-PAGE sample buffer and resolved on a 10% SDS-PAGE gel. The gel was transferred to a PVDF membrane and blotted with a 1:1000 dilution of affinity-purified rabbit anti-Best2 antibody B4947A, as described.[18]

Immunohistochemistry

Immunohistochemistry was performed as before[19] on unfixed, frozen sections (ABC kit with VIP as substrate; Vector Laboratories, Burlingame CA) with affinity-purified rabbit anti-Best2 antibody B4947A at a 1:500 dilution. Immunofluorescent staining of unfixed, frozen sections was performed as before[12] using a 1:50 dilution of the affinity-purified rabbit anti-Best2 antibody B4947A[12] and a CY3-conjugated goat anti-rabbit IgG antibody.

IOP Measurements

IOP was measured in the mice by cannulation of the anterior chamber as described by others,[20-22] with Avertin anesthesia (300 mg/kg injected intraperitoneally). In brief, the anterior chamber was cannulated with a borosilicate glass microneedle (1-mm outer diameter with a 50-μm inner diameter tip, beveled to 45°; Humagen, Charlottesville, VA) filled with Hanks' balance salt solution (HBSS) and connected to a pressure transducer (BLPR; World Precision Instruments, Sarasota, FL). The signal was amplified (Bridge8 amplifier; World Precision Instruments), converted from analog to digital (Iworx model 108 converter; CB Sciences, Dover, NH), and recorded (LabScribe software ver.1.6; CB Sciences, Dover, NH). IOP was recorded for a period of >90 seconds, and the IOP value determined from the average of each recording. Recordings were discarded if the variance during the recording period exceeded 1 mm Hg or did not immediately return to zero after withdrawal of the needle. All measurements were performed between 2 and 6 PM to avoid diurnal pressure variation. The apparatus was calibrated using a fluid reservoir the height of which could be adjusted to generate a series of known pressures. For experiments using timolol (0.5% solution; Bausch & Lomb, Tampa, FL) or brinzolamide (Azopt 1% solution; Alcon, Fort Worth, TX), 10 μL of solution was administrated topically to each eye 2 hours before cannulation.

Measurements of EVP (episcleral venous pressure) were performed as described by Aihara et al.[22] IOP was first measured as described earlier, after which the height of the saline-filled reservoir was adjusted to equal the IOP, and the stopcock between the transducer and reservoir was opened. The height of the reservoir was decreased 0.5 mm Hg (0.68 mm H_2O) per minute. EVP was determined as the pressure at which reflux of blood from collector channels into Schlemm's canal could be observed through a dissecting microscope. The reservoir was then returned to its original height, and the measurement repeated in the same eye. Differences in IOP and EVP between experimental groups were compared by t-test.

RESULTS

Generation of Mice with a Disrupted *Best2* Gene

The murine *Best2* gene was disrupted by replacing exons 1 and 2 and part of exon 3 with a promoterless LacZ and a neomycin-resistance gene cassette through homologous recombination (Fig. 1A). The *LacZ* gene contained a sequence encoding a nuclear localization signal. The disruption of the gene was confirmed by Southern blot analysis (Fig. 1B) and PCR (Fig. 1C). The $Best2^{-/-}$ mice were viable, grew normally, were fertile, and demonstrated no obvious physical or behavioral abnormalities.

Expression Profiling of *Best2*

The *Best2* gene is reportedly expressed in multiple mouse tissues and organs, including RPE, colon, testis, and nasal epithelia.[3,23] To determine whether we had generated a true null mutant, we performed RT-PCR on total RNA from colon and eye. As shown in Figure 2A, the 585-bp reaction product obtained from the $Best2^{+/+}$ and $Best2^{+/-}$ mice was absent from these organs in mRNA isolated from the $Best2^{-/-}$ mice. We used RT-PCR to scan additional mouse organs for *Best2* mRNA. As shown in Figure 2 and Table 1, positive results were obtained from multiple organs with bands for eye, colon, and nasal epithelium being strongest and most reproducible.

In the *Best2*-knockout mouse, the *Lac Z* gene was inserted into the *Best2* gene placing it under control of the endogenous *Best2* promoter. This method provided a second means of analysis of *Best2* expression in the $Best2^{-/-}$ and $Best2^{+/-}$ mice by using X-gal staining. As summarized in Table 1, of the tissues surveyed, only the colon and eye (Fig. 3) were consistently and strongly positive for X-gal staining. Nasal epithelia

FIGURE 2. The expression of *Best2* mRNA was probed using RT-PCR in multiple tissues. Initially, eye and colon were examined to validate that a true null mutant had been generated (**A**). A PCR product of the correct size (585 bp), representing *Best2* mRNA was present in eye and colon in the $Best2^{+/+}$ and $Best2^{+/-}$ mice, but not in the $Best2^{-/-}$ mice (**A**). Next other organs were probed for *Best2* mRNA expression (**B**). Weak bands for *Best2* were identified in hind brain, nasal epithelium, kidney, trachea, and lung. +control, mBest2 cDNA used as a template; −control, template omitted.
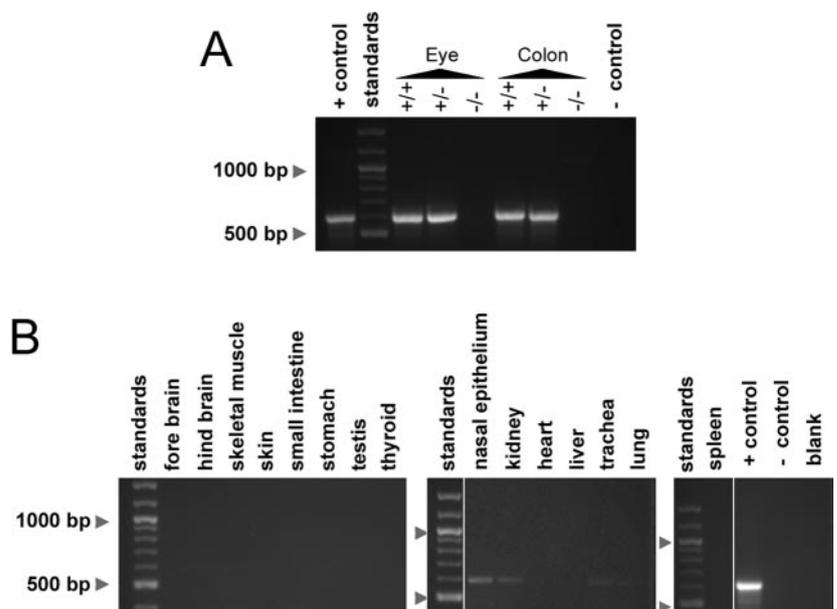
TABLE 1. Expression of Best2 in Mouse Organs/Tissues

Organ/Tissue	*Lac Z* Gene Expression*	RT-PCR	Protein Expression†
Eye (whole eye)	NA	+++	NA
Eye (ciliary body)	+++	ND	+++
Eye (RPE/choroid)	—	ND	—
Eye (other)	—	ND	—
Nasal epithelium	+/−	++	—
Fore brain	—	—	ND
Hind brain	—	+	ND
Liver	—	—	ND
Kidney	—	+	—
Heart	—	—	ND
Trachea	—	+	ND
Lung	—	+	ND
Skeletal muscle	—	—	ND
Spleen	—	—	ND
Skin	+/−	—	—
Colon	+++	+++	+++
Small intestine	—	—	ND
Stomach	—	—	ND
Testis	+/−	—	ND

ND, not done; NA, not applicable.

* Based on X-gal staining.

† Based on immunohistochemical staining.

were positive with prolonged incubation times; however, in every instance, the control (wild-type) nasal tissues were positive as well (data not shown). Results were ambiguous for testis, skin, and kidney. Lung, trachea, hind brain, and skeletal muscle, all positive by RT-PCR, were negative for X-gal staining. In colon, X-gal-positive cells appeared limited to a subset of epithelia and was absent from the base of the crypts. In the eye, we were surprised to find that X-gal staining was confined to NPE cells rather than the RPE as anticipated. No X-gal staining was observed in other ocular tissues.

Since we expected that *Best2* would be expressed in the RPE, we further examined its expression using RT-PCR of total RNA isolated from human RPE and ciliary body. Human tissues were used, because the larger eyes facilitate dissection of RPE
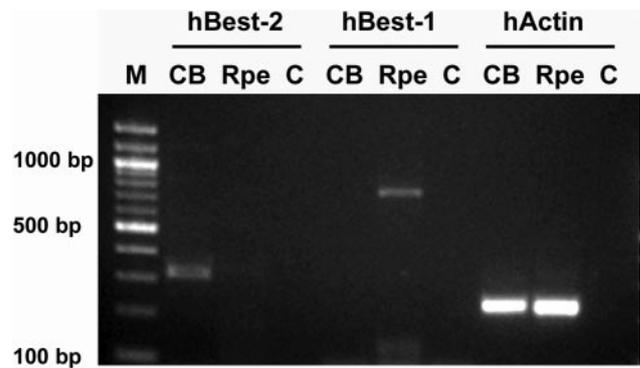

FIGURE 4. The expression of *Best2* in ciliary body (CB) and RPE was compared by RT-PCR. A band of 314 bp representing *BEST2* was observed only in CB and not RPE. As a control for tissue specificity and purity, *BEST1* expression was analyzed in these tissues as well. A band of 752 bp representing *BEST1*, which is uniquely expressed in the RPE, was detected only in RPE and not in CB. PCR performed with human actin (hActin) primers demonstrates that similar amounts of cDNA were used in each reaction. No reaction products were observed in lanes in which the template was omitted (**C**).

and ciliary body without cross-contamination. As shown in Figure 4, RPE was positive for *Best1* but not *Best2*, while ciliary body was positive for *Best2* and not *Best1*, confirming in the human eye, the expression pattern observed in mouse.

Localization of Best2 Protein

To examine the expression of Best2, we used an antibody raised against the C terminus of the murine protein.[12] The antibody recognizes recombinant mBest2 expressed in HEK 293 cells by Western blot as well as immunofluorescence (Figs. 5A, 5B). Similar to our findings with Best1,[15] we could not reliably detect Best2 in mouse tissues by Western blot. In colon, signal amplification with avidin-biotin was necessary to detect Best2 by immunohistochemistry (Figs. 5C, 5D). Immunohistochemical staining for Best2 using horseradish peroxidase labeled streptavidin and the substrate VIP to amplify the
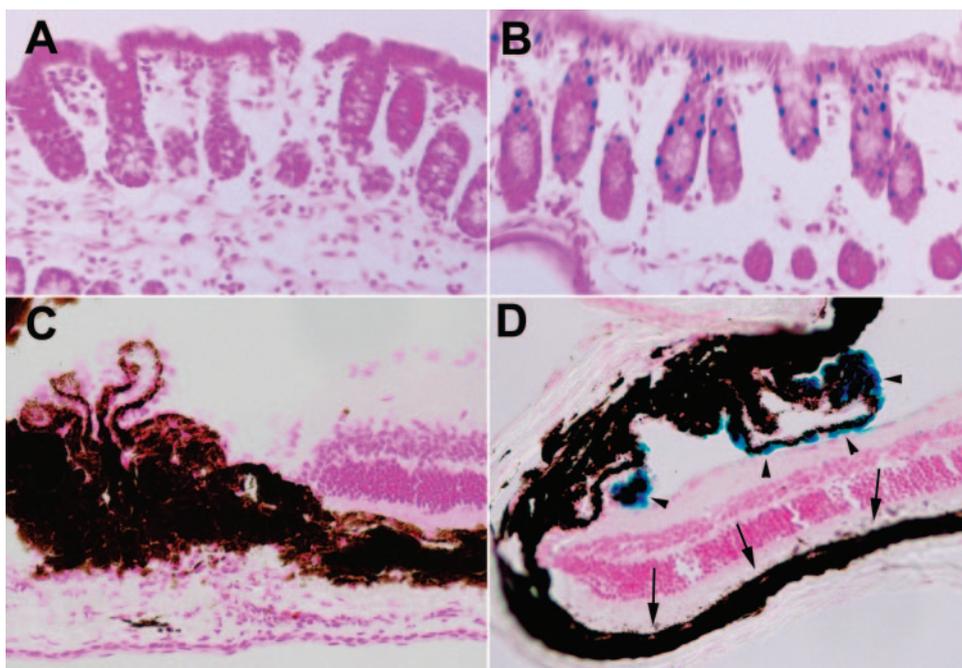

FIGURE 3. X-gal staining was used to identify tissues in which the *Best2* promoter functions. Of multiple tissues surveyed (Table 1), only colon (**A, B**) and eye (**C, D**) were consistently positive, as represented by the accumulation of a blue reaction product in the nuclei of a subset of colon epithelia (**B**) and in NPE cells (**D**, *arrowheads*). No reaction product was observed in the RPE (**D**, *arrows*). *LacZ* was present only in the *Best2*^{+/−} and *Best2*^{−/−} mice (**B, D**); we placed sections from the *Best2*^{+/+} mice (**A, C**) on the same slides as the control sections. No reaction product was observed in eye and colon in the *Best2*^{+/+} mice (**A, C**).
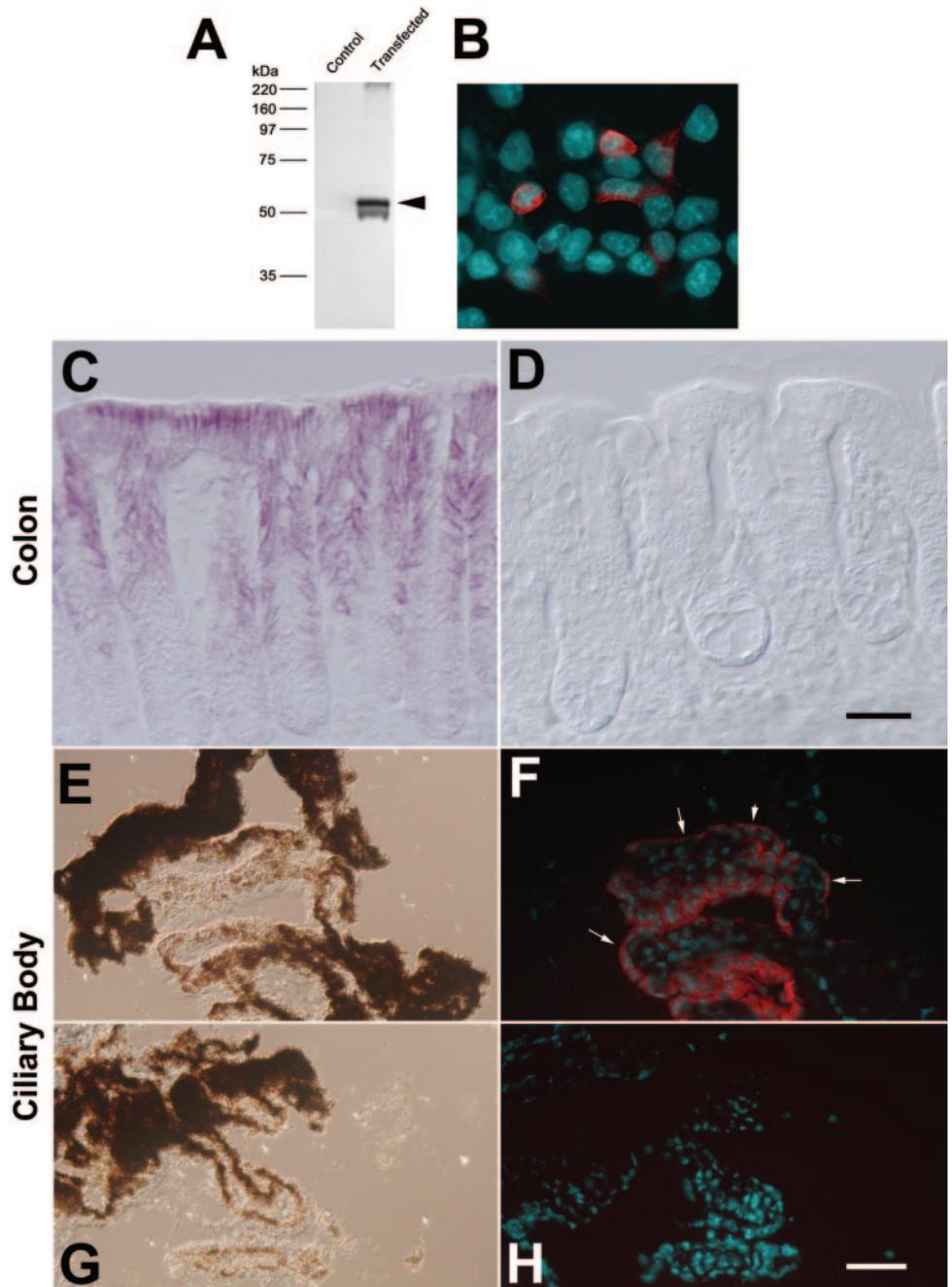
FIGURE 5. Expression of Best2 protein was probed with the antibody B4749A. Specificity was tested in transfected HEK293 cells by Western blot (**A**) and immunofluorescence (**B**). Best2 (*red*) was expressed in a subpopulation of cells. The expression of Best2 was probed by immunohistochemistry with antibody B4947A in colon from the $Best2^{+/+}$ (**C**) and $Best2^{-/-}$ (**D**) mice. (**C**) *Purple* VIP reaction product was deposited along the lateral borders of epithelia in the mid-to-luminal regions, but not at the base of the crypts in the $Best2^{-/-}$ mice. Reaction was absent from the $Best^{+/+}$ sections processed on the same slide. The localization of Best2 to the NPE of the ciliary body was examined by using immunofluorescence on unfixed cryosections of eyes (**F**, **H**). (**E**, **G**) DIC images of the sections shown in (**F**) and (**H**), respectively. *Red* staining for Best2 expression was observed only in the NPE of the $Best2^{+/+}$ mice (**F**) and not the NPE of the $Best2^{-/-}$ mice (**H**). In regions in which the NPE were in cross section, Best2 staining appeared to be associated only with the basal surface of the cells (**F**, *arrows*). Nuclei (*cyan*) in (**B**), (**F**), and (**H**) were stained with DAPI (4',6'-diamino-2-phenylindole). Scale bars, 60 μm.

signal revealed a dark-purple reaction product associated with the basolateral membranes of epithelial cells in the colon (Fig. 5C). No antibody staining for Best2 was observed in sections of colon from the $Best2^{-/-}$ mice stained simultaneously on the same slide (Fig. 5D). Of note, as observed with X-gal staining (Fig. 3B), antibody staining was absent from cells at the base of the crypts. We could not on the basis of immunohistochemical staining determine whether Best2 is expressed solely in goblet cells, as suggested by X-gal staining, since the goblet cells are intermingled with transporting epithelia, and staining of lateral membranes was most prominent.

In the eye, signal amplification was not necessary, and so we used immunofluorescence to localize Best2. Best2 was observed only in NPE cells (Fig. 5F). The protein appeared to be polarized along the basal membranes of the cells. No staining was observed in the RPE, even with signal amplification (not shown), and no staining was observed in sections from the $Best2^{-/-}$ mice stained

simultaneously on the same slide (Fig. 5H). These results agree with our observations obtained with X-gal staining.

We also examined nasal tissues for expression, by using immunohistochemistry with avidin-biotin signal amplification, but could not detect any Best2 reactivity (data not shown).

Phenotype Analysis of the $Best2^{-/-}$ Mice

The $Best2^{-/-}$ mice exhibited no obvious phenotypic abnormalities. Because Best2 was reported by other investigators to be expressed in nasal epithelia,[23] we assayed the mice for impaired olfactory responses. Mice were starved for 24 hours and then challenged to find hidden food. In this assay, mice with olfactory defects due to a disruption of the *Bbs2* gene were incapable of finding the food within a 10-minute period, whereas wild-type mice found it within 240 seconds.[24] The $Best2^{-/-}$ mice found the food in an average of 266 ± 144

TABLE 2. Mean IOPs in Control and Drug Treated *Best2*-Knockout Mice

	C57BL/6	*Best2*$^{+/+}$	*Best2*$^{+/-}$	*Best2*$^{-/-}$
Untreated	11.78 ± 0.22	11.73 ± 0.37	11.52 ± 0.44	10.56 ± 0.21
	n = 28	*n* = 12	*n* = 20	*n* = 39
Brinzolamide	10.51 ± 0.51	10.08 ± 0.33	9.56 ± 0.37	9.34 ± 0.34
	n = 11	*n* = 10	*n* = 12	*n* = 11
Timolol	10.53 ± 0.29	9.57 ± 0.22	9.48 ± 0.12	9.49 ± 0.18
	n = 10	*n* = 11	*n* = 11	*n* = 11

Data are mean ± SE (in mm Hg).

seconds (*n* = 10). Their performance was similar to that of their *Best2*$^{+/+}$ littermates, which found the food in 231 ± 141 seconds (*n* = 10). We conclude from this that *Best2*$^{-/-}$ mice have no significant olfactory deficit. We observed no obvious gastrointestinal distress in the mice. Despite the absence of expression of Best2 in colon, the mice did not exhibit diarrhea or any other obvious symptom of colon dysfunction.

The expression of *Best2* in the eye has been predicted.[3,4] While we anticipated on the basis of these prior studies that *Best2* would be expressed in RPE cells, we found that it was instead expressed in the NPE cells of the ciliary body. The ciliary epithelial cells play a critical role in the generation of aqueous humor. Since IOP is determined by the balance between aqueous humor secretion and outflow facility, we hypothesized that the disruption of *Best2* might affect IOP. We measured IOP in mice according to the methods of John et al.,[21] and Aihara et al.[22] in which a glass micropipette connected to a pressure transducer is inserted through the cornea and into the anterior chamber of the eye. Our wild-type C57BL/6 mice exhibited IOPs of 11.78 ± 0.22 (average ± SE, *n* = 28; Table 2) consistent with prior reports[22] of the use of this technique. The *Best2*$^{+/+}$ and *Best2*$^{+/-}$ littermates exhibited comparable IOPs that did not differ significantly (*P* = 0.979 and *P* = 0.989, respectively) from the C57BL/6 control group (Fig. 6A, Table 2), although there was more variability in the *Best2*$^{+/-}$ mice. In contrast, the *Best2*$^{-/-}$ mice exhibited significantly (*P* < 0.02) lower IOPs than did C57BL/6 mice or their *Best2*$^{+/+}$ and *Best2*$^{+/-}$ littermates (Fig. 6A, Table 2). Measurements of the EVP of the mice identified no differences between genotypes, with all mice exhibiting an EVP of 6.3 ± 0.4 mm Hg (average ± SD, *n* = 12). Because of the reduced IOP in the *Best2*$^{-/-}$ mice and its expression in NPE cells, we conclude that *Best2* probably contributes to the formation of aqueous humor.

To elucidate further the role of *Best2* in generating aqueous humor, we treated mice with either the carbonic anhydrase in-
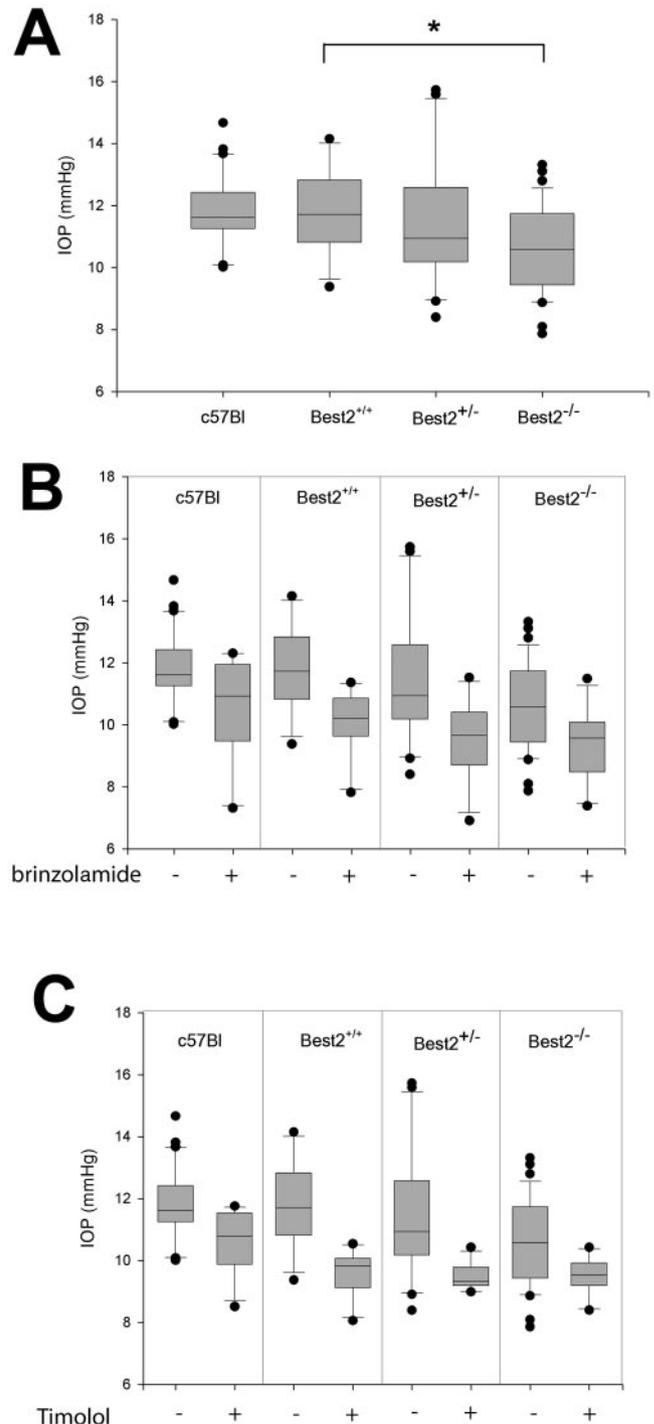

FIGURE 6. (A) The IOP of the C57BL/6 mice and *Best2*$^{-/-}$ mice along with their *Best*$^{+/-}$ and *Best*$^{+/+}$ littermates was determined and compared. A significantly diminished IOP (*) was observed in the *Best2*$^{-/-}$ mice (*n* = 39) versus the *Best2*$^{+/+}$ littermates (*n* = 11), *Best2*$^{+/-}$ littermates (*n* = 20), and C57BL/6 mice (*n* = 31). Each graph contains box plots in which the *line* within the box marks the median IOP, and the *boundary* of the box farthest from 0 indicates the 75th percentile. Error bars above and below the boxes indicate the 90th and 10th percentiles, respectively. (B) The effect of the carbonic anhydrase inhibitor brinzolamide was determined and compared to the general population of untreated mice of each strain/genotype. Brinzolamide was significantly more effective in lowering IOP in the *Best2*$^{+/-}$ mice (*n* = 12, *P* < 0.01) than other genotypes and reduced IOP in the *Best2*$^{-/-}$ mice (*n* = 11, *P* < 0.01) to a lower level than in C57BL/6 (*n* = 10, *P* < 0.02) or the *Best2*$^{+/+}$ littermates (*n* = 10, *P* < 0.01). (C) Timolol caused a significant (*P* < 0.005) reduction in all groups (*n* = 11 in each timolol-treated group), with the median being similar in the *Best2*$^{+/+}$, *Best2* $^{+/-}$, and *Best2*$^{-/-}$, mice. IOP was less efficiently lowered by timolol in the C7BL/6 mice.

hibitor brinzolamide or the β-blocker timolol. Timolol has been shown to be effective in lowering IOP in mice,[25] as have carbonic anhydrase inhibitors,[25] and both drugs are currently used to lower IOP in humans with glaucoma. Brinzolamide was effective in lowering IOP in all mice tested (Fig. 6B, Table 2). Treatment with brinzolamide resulted in reduction to a lower IOP in the $Best2^{+/-}$ and $Best2^{-/-}$ mice than in the C57BL/6 or $Best2^{+/+}$ mice. Of interest, despite the mean IOP being similar in the $Best2^{+/+}$ and $Best2^{+/-}$ mice, brinzolamide was more effective in reducing IOP in the $Best2^{+/-}$ mice, reducing the overall pressure to the same level as observed in the $Best2^{-/-}$ mice treated with the drug (Fig. 6B, Table 2); approximately 1 mm Hg lower than was observed in the C57BL/6 or $Best2^{+/+}$ mice. In contrast, timolol, which lowered IOP significantly ($P < 0.005$) in the C57BL/6 and $Best2^{+/+}$ mice, brought the IOP to the same level in the $Best2^{+/-}$ and $Best2^{-/-}$ mice (Fig. 6C, Table 2), making it less effective in lowering IOP in the $Best2^{-/-}$ mice, and suggesting that Best2 plays a role downstream of the $\beta2$ adrenergic receptor that is the presumptive target of timolol.

DISCUSSION

Data on the physiological role of any bestrophin in any tissue are sparse. Most of the available data are derived from *Best1*, for which we have previously disrupted the gene in mice[15] and which when mutated can cause several blinding diseases. None of these disorders is associated with nonocular abnormalities. In the present study, we sought to further our knowledge on the role of bestrophins by disrupting the *Best2* gene in mice. Similar to our observations in $Best1^{-/-}$ mice, we found that the $Best2^{-/-}$ mice exhibited no obvious defects. Using a combination of methods, we found that the gene and protein are clearly expressed only in the NPE cells of the ciliary body and in epithelial cells of the colon.

The restricted expression of Best2 observed in this study is similar to the restricted expression that we have reported for Best1, which indicates that the protein is expressed only in RPE cells.[9,26] These data reinforce the idea that bestrophins are expressed in very specific cell types and are not widely distributed in tissues throughout the body. The limited expression of Best2 led us to identify an important ophthalmic phenotype: a significant reduction in the IOP of the $Best2^{-/-}$ mice and differences among genotypes with regard to sensitivity to drugs that affect the aqueous inflow pathway. These results suggest that Best2 plays a role in the generation of intraocular pressure, most likely by participating in the formation of aqueous humor. The data also suggest that Best2 is a potential therapeutic target for the treatment of glaucoma. Of note, the human *BEST2* gene is located on the short arm of chromosome 19 near a strong glaucoma locus identified by sib pair analysis.[27] Based on our findings, *BEST2* represents a potential candidate for the glaucoma gene at this locus. Our data suggest that loss of function or diminished expression of BEST2 are protective against glaucoma and that BEST2 gain of function mutations predispose to glaucoma.

How might Best2 affect IOP? IOP is determined from the sum of the EVP plus the ratio of aqueous humor formation and its drainage through the outflow facility. Since EVP was similar in all genotypes studied, Best2 must play a role in either inflow or outflow. We favor scenarios in which Best2 affects aqueous formation because of its localization on the basal surface of the NPE, its ability to generate or regulate Cl^- conductances, and the differential effects across *Best2* genotypes of drugs altering aqueous inflow (Figs. 6B, 6C). It has long been recognized that water transport across the ciliary epithelium is coupled to the transepithelial transport of Cl^- by the NPE.[28-30] NPE cells secrete Cl^- via channels in their basal plasma membrane. Our

data indicate that Best2 is present at the NPE basal plasma membrane, and so the simplest explanation is that Best2 is one of at least three species of Cl^- channels that have been described in the NPE.[28] The absence of one species of Cl^- channel may result in a diminished IOP similar our observations. Although there is no evidence that NPE Cl^- transport is Ca^{2+} sensitive, Best2 Cl^- transport is Ca^{2+} regulated.[12] However, the apparent affinity for Ca^{2+} is high so that a considerable fraction of Best2 channels are active at "resting" intracellular Ca levels.[12] Furthermore, Best2 Cl^- channel activity is also volume sensitive.[27] Some Cl^- channels in the basal NPE membrane are volume sensitive,[31] and some models for fluid secretion by ciliary epithelia invoke volume-regulated anion channels. Cl^- transport in the NPE is coupled to HCO_3^- transport, which is affected by carbonic anhydrase inhibitors. The altered sensitivity of the $Best2^{+/-}$ and $Best2^{-/-}$ mice to brinzolamide (Fig. 6B) is consistent with this idea. The β-blocker timolol brought IOP to the same level in all mice tested (Fig. 6C). Timolol affects adrenergic signaling via $\beta2$ adrenergic receptors in NPE cells.[32,33] This pathway is thought to govern inflow by regulating the number of Cl^- channels present in the basal membrane of the NPE,[28] and so it is possible that Best2 represents a population of channels that can be mobilized in response to adrenergic signaling.

Another possible function for Best2 in the inflow pathway is as an antagonist to Ca^{2+} signaling, as we have proposed for Best1. According to Mitchell et al.,[34] ATP stimulates P2Y2 receptors in ciliary pigmented epithelial (PE) cells and triggers Ca^{2+} release. PE cells release ATP due to cell swelling, which results in activation of a hypothesized Ca^{2+}-dependent, negative-feedback loop sending Cl^- into the stroma.[28,34] But why then is Best2 on the NPE and not the PE? Perhaps it is the governor of the negative feedback loop or maybe it senses Cl^- flux across the NPE basal membrane and alters Ca^{2+} signaling sensitivity to prevent this negative feedback loop from overtaking the positive flow of aqueous humor. In its absence, the failure to regulate Ca^{2+} properly could result in a faster move toward recycling of Cl^- and diminished aqueous production. According to this scenario, the apparent amplification of the brinzolamide effect would be via changes in pH, perhaps via the Na^+/H^+ exchanger,[35,36] with downstream effects via intracellular pH on overall Ca^{2+} signaling.

Although further studies are needed to clarify the role of Best2 in the generation of IOP, it is clear that Best2 represents a new potential target for the development of drugs to lower IOP. Because Best2-deficient mice continue to respond to drugs that have been traditionally used to lower IOP in patients with glaucoma, a drug that blocks Best2 activity could function synergistically with currently available drugs expanding the repertoire of therapies available to treat this blinding disease.

References

1. Hartzell C, Qu Z, Putzier I, Artinian L, Chien LT, Cui Y. Looking chloride channels straight in the eye: bestrophins, lipofuscinosis, and retinal degeneration. *Physiology*. 2005;20:292–302.
2. Marmorstein AD, Kinnick TR. Focus on molecules: bestrophin (Best-1). *Exp Eye Res*. 2006;85:423–424.
3. Kramer F, Stohr H, Weber BH. Cloning and characterization of the murine Vmd2 RFP-TM gene family. *Cytogenet Genome Res*. 2004; 105:107–114.
4. Stohr H, Marquardt A, Nanda I, Schmid M, Weber BH. Three novel human VMD2-like genes are members of the evolutionary highly conserved RFP-TM family. *Eur J Hum Genet*. 2002;10:281–284.

5. Cross HE, Bard L. Electro-oculography in Best's muscular dystrophy. *Am J Ophthalmol.* 1974;77:46–50.

6. Deutman AF. Electro-oculography in families with vitelliform dystrophy of the fovea. *Br J Ophthalmol.* 1969;81:305–316.

7. Gallemore RP, Hughes BA, Miller SS. Light-induced responses of the retinal pigment epithelium. In: Marmor MF, Wolfensberger TJ, ed. *The Retinal Pigment Epithelium.* New York: Oxford University Press; 1998:175–198.

8. Sun H, Tsunenari T, Yau KW, Nathans J. The vitelliform macular dystrophy protein defines a new family of chloride channels. *Proc Natl Acad Sci USA.* 2002;99:4008–4013.

9. Stanton JB, Goldberg AF, Hoppe G, Marmorstein LY, Marmorstein AD. Hydrodynamic properties of porcine bestrophin-1 in Triton X-100. *Biochim Biophys Acta.* 2006;1758:241–247.

10. Milenkovic VM, Rivera A, Horling F, Weber BH. Insertion and topology of normal and mutant bestrophin-1 in the endoplasmic reticulum membrane. *J Biol Chem.* 2007;282:1313–1321.

11. Tsunenari T Sun H, Williams J, et al. Structure-function analysis of the bestrophin family of anion channels. *J Biol Chem.* 2003;278:41114–41125.

12. Qu Z, Fischmeister R, Hartzell C. Mouse bestrophin-2 is a bona fide Cl(−) channel: identification of a residue important in anion binding and conduction. *J Gen Physiol.* 2004;123:327–340.

13. Qu Z, Hartzell C. Determinants of anion permeation in the second transmembrane domain of the mouse bestrophin-2 chloride channel. *J Gen Physiol.* 2004;124:371–382.

14. Qu Z, Chien LT, Cui Y, Hartzell HC. The anion-selective pore of the bestrophins, a family of chloride channels associated with retinal degeneration. *J Neurosci.* 2006;26:5411–5419.

15. Marmorstein LY, Wu J, McLaughlin P, et al. The light peak of the electroretinogram is dependent on voltage-gated calcium channels and antagonized by bestrophin (best-1). *J Gen Physiol.* 2006;127:577–589.

16. Rosenthal R, Bakall B, Kinnick T, et al. Expression of bestrophin-1, the product of the VMD2 gene, modulates voltage-dependent Ca2+ channels in retinal pigment epithelial cells. *FASEB J.* 2006;20:178–180.

17. Wu J, Marmorstein AD, Striessnig J, Peachey NS. Voltage-dependent calcium channel CaV1.3 subunits regulate the light peak of the electroretinogram. *J Neurophysiol.* 2007;97:3731–3735.

18. Marmorstein LY, Ouchi T, Aaronson SA. The BRCA2 gene product functionally interacts with p53 and RAD51. *Proc Natl Acad Sci USA.* 1998;95:13869–13874.

19. Bakall B, Marmorstein LY, Hoppe G, Peachey NS, Wadelius C, Marmorstein AD. Expression and localization of bestrophin during normal mouse development. *Invest Ophthalmol Vis Sci.* 2003;44:3622–3628.

20. Husain S, Whitlock NA, Rice DS, Crosson CE. Effects of latanoprost on rodent intraocular pressure. *Exp Eye Res.* 2006;83:1453–1458.

21. John SW, Hagaman JR, MacTaggart TE, Peng L, Smithes O. Intraocular pressure in inbred mouse strains. *Invest Ophthalmol Vis Sci.* 1997;38:249–253.

22. Aihara M, Lindsey JD, Weinreb RN. Aqueous humor dynamics in mice. *Invest Ophthalmol Vis Sci.* 2003;44:5168–5173.

23. Pifferi S, Pascarella G, Boccaccio A, et al. Bestrophin-2 is a candidate calcium-activated chloride channel involved in olfactory transduction. *Proc Natl Acad Sci USA.* 2006;103:12929–12934.

24. Nishimura DY, Fath M, Mullins RF, et al. Bbs2-null mice have neurosensory deficits, a defect in social dominance, and retinopathy associated with mislocalization of rhodopsin. *Proc Natl Acad Sci USA.* 2004;101:16588–16593.

25. Avila MY, Carre DA, Stone RA, Civan MM. Reliable measurement of mouse intraocular pressure by a servo-null micropipette system. *Invest Ophthalmol Vis Sci.* 2001;42:1841–1846.

26. Marmorstein AD, Marmorstein LY, Rayborn M, Wang X, Hollyfield JG, Petrukhin K. Bestrophin, the product of the Best vitelliform macular dystrophy gene (VMD2), localizes to the basolateral plasma membrane of the retinal pigment epithelium. *Proc Natl Acad Sci USA.* 2000;97:12758–12763.

27. Duggal P, Klein AP, Lee KE, Klein R, Klein BE, Bailey-Wilson JE. Identification of novel genetic loci for intraocular pressure: a genomewide scan of the Beaver Dam Eye Study. *Arch Ophthalmol.* 2007;125:74–79.

28. Do CW, Civan MM. Basis of chloride transport in ciliary epithelium. *The J Membr Biol.* 2004;200:1–13.

29. Shahidullah M, Wilson WS, Yap M, To CH. Effects of ion transport and channel-blocking drugs on aqueous humor formation in isolated bovine eye. *Invest Ophthalmol Vis Sci.* 2003;44:1185–1191.

30. Kong CW, Li KK, To CH. Chloride secretion by porcine ciliary epithelium: new insight into species similarities and differences in aqueous humor formation. *Invest Ophthalmol Vis Sci.* 2006;47:5428–5436.

31. Do CW, Peterson-Yantorno K, Civan MM. Swelling-activated Cl⁻ channels support Cl⁻ secretion by bovine ciliary epithelium. *Invest Ophthalmol Vis Sci.* 2006;47:2576–2582.

32. Avila MY, Stone RA, Civan MM. Knockout of A3 adenosine receptors reduces mouse intraocular pressure. *Invest Ophthalmol Vis Sci.* 2002;43:3021–3026.

33. McLaughlin CW, Peart D, Purves RD, et al. Timolol may inhibit aqueous humor secretion by cAMP-independent action on ciliary epithelial cells. *Am J Physiol.* 2001;281:C865–C875.

34. Mitchell CH, Carre DA, McGlinn AM, Stone RA, Civan MM. A release mechanism for stored ATP in ocular ciliary epithelial cells. *Proc Natl Acad Sci USA.* 1998;95:7174–7178.

35. Avila MY, Seidler RW, Stone RA, Civan MM. Inhibitors of NHE-1 Na⁺/H⁺ exchange reduce mouse intraocular pressure. *Invest Ophthalmol Vis Sci.* 2002;43:1897–1902.

36. Counillon L, Touret N, Bidet M, et al. Na+/H+ and Cl-/HCO3-antiporters of bovine pigmented ciliary epithelial cells. *Pflugers Arch.* 2000;440:667–678.